Collapse characterization and shock mitigation by elastomeric metastructures

Peter Vuyk, Ryan L. Harne *

Department of Mechanical and Aerospace Engineering, The Ohio State University, Columbus, OH, 43210, United States of America

ARTICLE INFO

ABSTRACT

Viscoelastic metastructures made with elastomeric polymers are recently suggested as solutions for shock mitigation and crash absorption. In these investigations, the mechanical properties are used as proxy indicators of capabilities to suppress energy transfer under such dynamic load conditions. Yet, recent high speed video studies revealed a startling disconnect between quasi-static and dynamic behavior in metastructures having internal beam networks due to the coupled local–global dynamics that are not triggered during quasi-static load cycles. This research undertakes an extensive high speed video data collection synchronized with force measurements to reveal the influences that govern transient shock mitigation properties in elastomeric metastructures. Despite an intuitive advantage of prolonging the collapse behavior through material design, it is conclusively found that unimodal collapse of the metastructure cross-section is the most effective mechanism to mitigate shock amplitude, prolong the duration of the transmitted force, and to reduce the impulse passed through the media. This research may specifically inspire the next generation of elastomeric, reusable shock damping materials.

© 2020 Elsevier Ltd. All rights reserved.

1. Main text

Materials with strategically designed internal architectures cultivate a multitude of non-natural mechanical properties at bulk length scales [1]. The subwavelength microstructures exert passive control over elastic wave propagation, giving rise to exceptional dynamic phenomena including elastic and acoustic bandgaps [2,3], cloaking [4,5], topological edge states [6,7], and non-reciprocal behavior [8,9]. When the internal structures are respectfully nearer in dimensions to the wavelengths that pass through the engineered media, such metamaterials are often referred to as metastructures. For metastructures, the material behavior is strongly influenced by boundaries, asymmetry, and the specific distributions of inertial, elastic, and dissipative constituents [10–14]. Because of these factors, the demonstration of non-periodic behavior from periodically-assembled metastructures [15,16] encourages attention to the interplay between local and global mechanisms of strain energy transfer to understand correlations among design parameters and observable dynamic behavior.

Metastructures are especially proposed for impact energy absorption [15,17–20], enabling future applications of packaging, protective systems, and crash mitigation. To substantially tailor or diminish a transmitted pulse, the bulk material from which

a metastructure is fabricated should possess a viscoelastic relaxation time near the order of the time of pulse application [21]. Recent metastructures fabricated using thermoplastic polymers, such as additively manufactured materials [22–25], exhibit long relaxation times due to operation below glass transition temperature T_g [26]. As a result, thermoset elastomers, that are often used above T_g and exhibit less plasticity and greater reversibility, are often suitable materials for shock absorption [21]. On the other hand, emerging evidence suggests that thermoset-based metastructures are capable of highly non-affine mechanical properties [16,17,27] and non-intuitive dynamic behavior [15,28], emphasizing a need to scrutinize the factors that govern such characteristics on the time scales of the microstructural material response.

In this report, we consider a model elastomeric metastructure fabricated using thermoset silicone rubber where the internal microstructure contains vertical beams separated by horizontal elastomer beams, Fig. 1(a). Local buckling, multi-directional stress transfer, and local vibrations are evident in the metastructure when subjected to shock [15]. This suggests intricate connections among local and global dynamic response to result in macroscopic behavior. In this report, we seek to uncover mechanisms that enable control of the transmitted transient shock through elastomeric metastructures. Through high speed video, digital image correlation, and comparison among material variants, we find that shock stress transfer, diffusion, and dissipation in the metastructures are governed by gradients in the microstructure

---
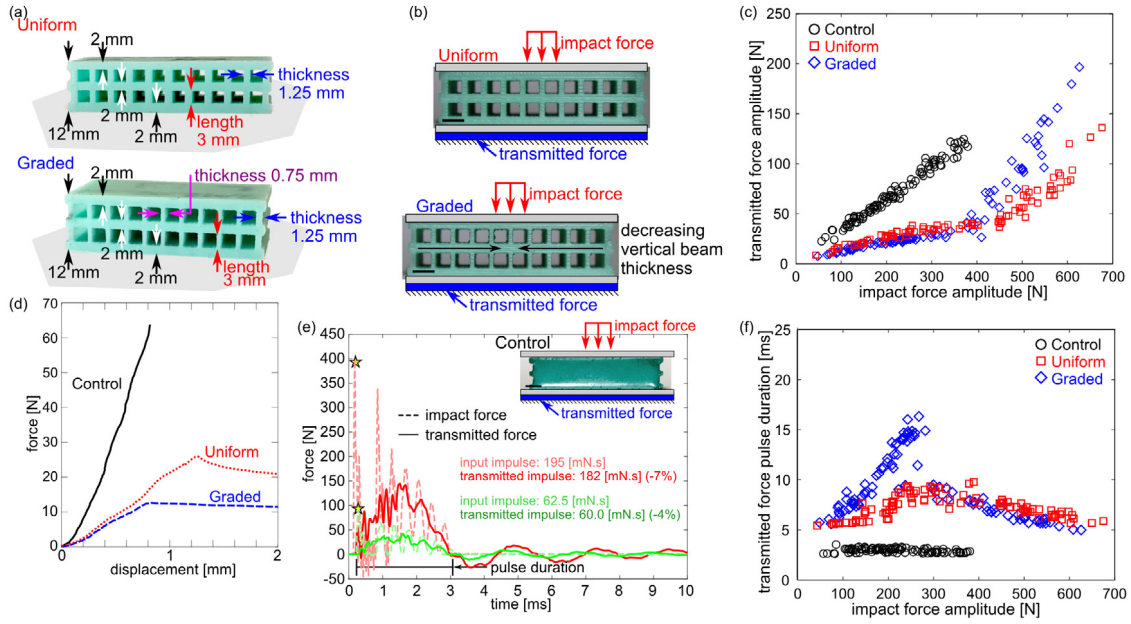
Fig. 1. (a) Metastructure geometry. Sample depth of constant cross-section is 25 mm. (b) Impact experimental protocol. (c) Transmitted force amplitude for change in impact force amplitude. (d) Mechanical properties in uniaxial compression. (e) Transient response of impact and transmitted forces for Control sample. (f) Transmitted pulse duration change for impact force amplitude.

material design that directly control a sequential metastructure collapse and strain distribution. The following report synthesizes the investigations and findings, and creates a fundamental understanding of strategies by which shock may be tailored and mitigated in new classes of elastomeric materials.

The metastructures here are fabricated from Shore 15A durometer silicone rubber (Smooth-On Mold Star 15S, Macungie, PA). The vertically aligned beams in the sample have uniform thickness to length ratio 0.42 thus earning the name of the "Uniform" metastructure. When subjected to uniaxial compression, a lateral buckling of the vertical beams in the metastructure may occur leading to elastic energy mitigation [15]. In this event, a bifurcation occurs between left and right lateral motion of the central horizontal beam [15]. Yet, the modulation of shock pulses through these metastructures is far less intuitive that the correspondence of mechanical properties and dynamic stiffness. The protocol to evaluate shock transmission in this work is to simultaneously record high speed video and the input and output force data streams when the metastructure is struck by an impact hammer (PCB 086C03, Depew, NY) on a force transduction plate (PCB 208C03). The high speed Video 1 exemplifies the local and global deformation of the Uniform metastructure when struck by this technique, schematically shown in Fig. 1(b).

In addition to the Uniform sample, a metastructure termed "Graded" is also fabricated and tested. The thickness to length ratios of the vertical beams in the Graded metastructure vary linearly from 0.42 at the periphery to 0.25 at the center. Although not reported here for sake of brevity, 20 metastructure samples are fabricated with vertical beam thicknesses and gradients varied around the parameters used for the Uniform and Graded materials. The results presented in this report for the Uniform and Graded samples help uncover relationships among metastructure design, material deformation, and shock transmission that are representative of the results corresponding to the whole range of samples. A solid elastomer material termed "Control" is also molded using the same silicone rubber in the same net dimensions as the Uniform.

The samples are subjected to impact forces using the experimental protocol. The resulting amplitudes of transmitted force as

functions of impact force amplitudes are presented in Fig. 1(c). The Control exhibits a linear proportionality between impact and transmitted forces, where the proportionality constant is related to the mass per unit area [29]. Comparatively, the transmitted force per impact force is much less for both the Uniform and Graded metastructures. In Fig. 1(c), around 350 N for the Graded and 400 N for the Uniform metastructures, the transmitted force increases notably with further increase in impact force. The mechanical properties of the samples in Fig. 1(d) show buckling behavior for the Graded and Uniform samples respectively around 13 N and 27 N. These are much smaller forces than the impact force amplitudes at which the proportionality of transmitted force deviates. Considering the Video 1 for the Uniform sample subjected to a 370 N impact force, it is evident (and will be confirmed through this report) that the change of slope in transmitted force is related to a total compaction of the metastructure voids caused by extreme collapse resulting from large amplitude impact force.

Reduced amplitude of the pulse, prolonged pulse duration, and net reduction of the total impulse (the integral of the transmitted force) are important factors in the development of protective materials [30,31]. In fact, the amplitude and duration of transmitted force are related through the conservation of momentum while the reduction of the impulse is caused by non-conservative mechanisms such as damping and energy sink phenomena [32]. Fig. 1(e) reveals that the Control sample reduces the transmitted force from the input force amplitude but does not influence the duration of the pulse. Here, we define the pulse duration as the time elapsed from the initial rise of the transmitted force to the time where the force becomes negative and oscillations due to whole body vibration occur, Fig. 1(e). The impact pulse duration is approximately 250 μs (the subsequent input oscillations correspond to reverberant longitudinal waves through the material thickness [15]) while the Control sample passes a 3 ms duration pulse. Fig. 1(f) confirms that the Control sample leads to an unchanging pulse duration despite wide range of impact force amplitudes. By contrast, the metastructures exert substantial control over the duration of the pulse. The Fig. 1(f) shows that the Uniform metastructure may result in a pulse of nearly
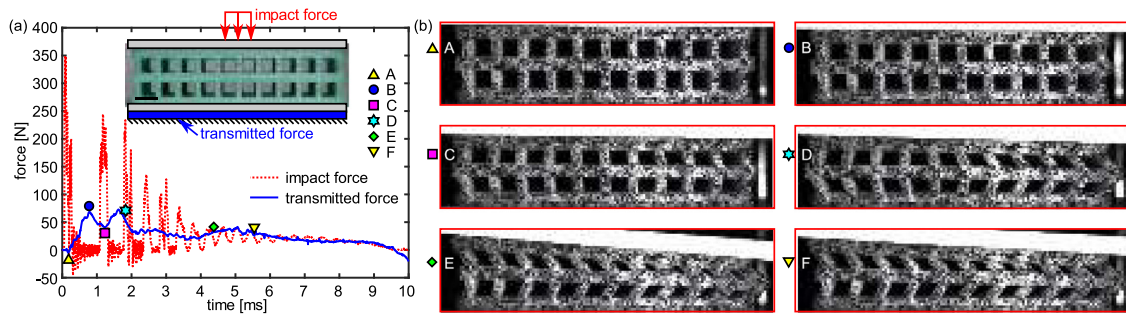
Fig. 2. Transient deformation behavior of Uniform metastructure subjected to 370 N impact force. (a) Impact and transmitted force in time with labels to denote the corresponding visual snap-shots shown in (b).

10 ms while the Graded metastructure can prolong the pulse to nearly 17 ms. Despite suggestions in previous research that impact energy dissipation in metastructures may be characterized through evaluation of mechanical properties [19,33,34], these first observations on shock measurements in Fig. 1 reveal the lack of correlation between quasi-static and high-rate behavior in viscoelastic, dissipative metastructures that will be illuminated through the investigations of this report.

Recent research introduced digital image correlation (DIC) to study the deformation characteristics of elastomeric materials subjected to shock [15]. On the other hand, the prior work [15] did not establish relationships between the deformation profiles and the shock transmission transients, which essentially govern shock mitigation. Here, the results in Fig. 2 create a first understanding of the sequential and local deformation characteristics that culminate in instantaneous shock transmission. For the Uniform sample, the Video 1 exemplifies that local buckling, cascading and synchronization, and bifurcation transition all contribute to the deformation of the Uniform cross-section when subjected to moderate amplitude shock.

Fig. 2(a,b) relates these behaviors with the associated transient shock transmission. Shortly after the impact, a compression of the material exhibits macroscopic positive Poisson's ratio due to net bulging that extends from the yellow triangle (A) to the blue circle (B), by which moment the transmitted force is maximized, Fig. 2(a,b). After the instant B, the material exhibits bimodal lateral buckling of the vertically oriented elastomeric beams and subsequent reduction of transmitted force up until the time indicated by the magenta square (C). A vertical beam near the center of the material cross-section does not buckle in this sequence and instead bulges while being laterally stretched by the central horizontal segment, Fig. 2(b). The transmitted force rises again until the moment in time in Fig. 2(a) labeled with the cyan hexagon (D) that corresponds to the beginning of the vertical beam cascade from right to left in the material cross-section. The cascading represents a transition through bifurcation of the vertical beams, from a left-ward buckled state to a right-ward buckled state. Such successive buckling is caused by the transmitted stress in the central horizontal elastomer segment and represents a lower energy state to pass towards than continued bimodal buckling [23,35]. After cascading completes and the vertical beams are synchronized in right-ward buckled states, the material begins to compact, such as that time instant shown by the green diamond (E) in Fig. 2(a,b). The compaction period continues until all horizontal beam segments contact the lateral beams, or until the impact load is removed, such as the moment labeled by the yellow triangle (F). Additional studies reported next consider the case of full compaction

The digital image correlation (DIC) method is used to help illuminate the relationships among metastructure internal geometry, deformation behavior, and stress transfer that may explain

the unique shock transmission characteristics found in Fig. 1(c,f). The molding process of the metastructure includes preparing one cross-section surface with a powder of carbon black. The speckling pattern created by this approach is empirically optimized for sake of the specific length scales of the materials and considering the high speed camera (Photron FastCam SA-X2) and lens (Nikon AF-S DX NIKKOR 35 mm f/1.8) employed in the data collection. The hammer impact and image capture are synchronized by a triggering pulse that registers the onset of the hammer impact. The impact event is lit by a triggered activation of an intense light (Nitecore Concept 1, 1800 Lumen) focused on the metastructure cross-section. Recordings at 50,000 frames per second are taken for 500 ms for each hit. DIC is then performed on the images using a MATLAB toolbox over the images cropped as seen in the videos and figures of this report. The DIC process uses 11 pixels subset size and step size of 2 pixels, while the correlation occurs serially over all acquired images with the first frame as the reference, due to large deformation. Thousands of hits are taken to obtain the data reported here and the practice is refined to ensure repeatability. Pixel deformation and the Green-Lagrangian strain components of x-normal E_{xx}, y-normal E_{yy}, and shear strain E_{xy} are computed using the MATLAB toolbox and are shown in the representative DIC images and videos. The high speed video recordings confirm that compaction events of the metastructures (if present) occur in the right-ward direction, despite near perfectly centered and normal-incidence impacts. The seemingly biased compaction has been found to be due to the small, but non-zero, lateral force component from the striking force hammer transducer that causes the collapse bifucation to result in right-ward compaction behavior. Yet, important to understand the transmitted shock characteristics, the origins and significance of the specific deformations of the metastructures are scrutinized here.

Fig. 3 presents the sequence of deformation profiles for the Uniform and Graded metastructures when subjected to impact forces around 340 N. Labels are given in the transient responses of transmitted force in Fig. 3(a) that correspond to the Uniform and Graded deformations shown in Fig. 3(b,c), respectively. The x-normal strain E_{xx}, shear strain E_{xy}, and y-normal strain E_{yy} are shown in descending rows in Fig. 3(b,c). Due to the large observed range of absolute strain, the DIC contours in Fig. 3(b,c) are presented as magnitudes normalized per strain component peak per metastructure sample. In other words, the E_{xx} strain for the Uniform metastructure is comparable to itself among the UA, UB, and UC times, yet is neither comparable to the E_{xy} strain normalization nor comparable to results for the Graded metastructure.

Despite the near identical impact force amplitudes, the transient transmitted forces through the Uniform and Graded metastructures bear little similarity, Fig. 3(a). The bimodal behavior of collapse prior to cross-section cascading to synchronize the
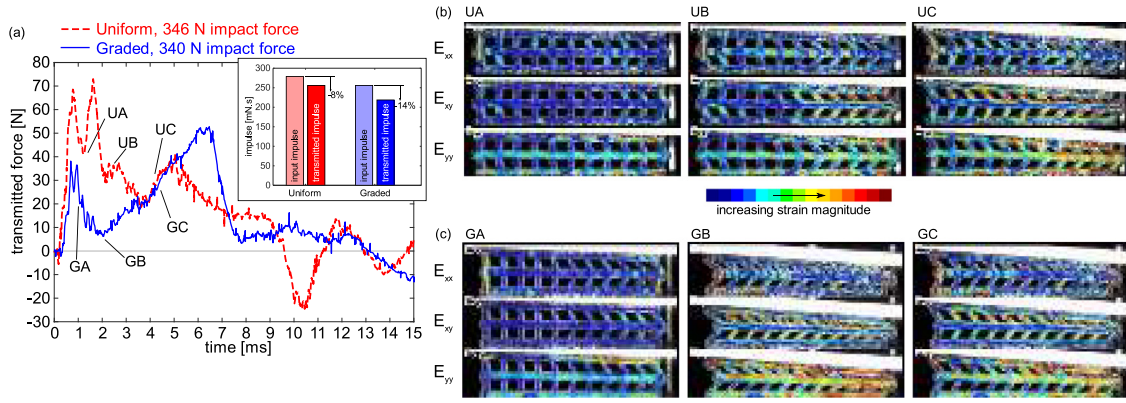
Fig. 3. (a) Transient transmitted force through Uniform and Graded metastructures. Inset shows the impulse reduction per sample. DIC results of strain magnitude components for (b) Uniform and (c) Graded metastructures.

vertical beam buckling is shown again through the Uniform sample DIC results in Fig. 3(b). The resistance to unimodal buckling results in little shear and y-normal strain through the material cross-section until the cascading event locks in the synchronous orientation of vertical beam buckling. By contrast, the Graded metastructure begins to immediately exhibit unimodal buckling once the brief period of linear elastic compression ends around 1 ms after impact, label GA in Fig. 3(a,c). As such, by just 2 ms after the shock application, the Graded metastructure transfers the applied longitudinal stress to shear and y-normal strain of the vertical beams, label GB Fig. 3(a,c). By labels UC and GC in Fig. 3, the metastructures each exhibit a period where the vertical beams laterally buckle in a synchronous fashion since the materials continue to be respectively compressed by the incident impulse.

The pulse durations are evident in Fig. 3(a) by the times at which the transmitted forces cross 0 N: around 9.5 ms for the Uniform and around 13 ms for the Graded metastructures. The inset of Fig. 3(a) shows that the Uniform metastructure reduces the input impulse by 8% compared to 14% by the Graded metastructure. Given the distinct deformation behaviors of the cross-section for similar applied shocks, it is evident that the propensity for the Graded metastructure geometry to support unimodal collapse after the onset of shock is a means by which the compaction sequence may be induced earlier. The compaction of the Graded metastructure cross-section induces large shear and y-normal strain in the vertical beams at times earlier than the same strain components are increased in the Uniform metastructure. These results therefore show that the compaction sequence associated with unimodal buckling is a means to dissipate greater shock energy than attempts to prolong buckling by bimodal deformation. Moreover, as these results reveal, the bimodal buckling trend for the Uniform metastructure actually reduces pulse duration. The Videos 2 and 3 show these trends with the impact and transmitted forces synchronized with the DIC image progression.

The extensibility of such relationships among metastructure cross-section design, deformation behavior, and resulting adaptation of shock transmission is tested through the results of Fig. 4. Here, Fig. 4(a) shows the transmitted forces for incident impacts around 190 N while Fig. 4(b,c) show the resulting DIC strain profiles for a time approximately 2.5 ms after impact application for the Uniform and Graded metastructures, respectively. For this amplitude of impact force, Fig. 1(f) shows that the Graded metastructure exhibits much longer pulse duration than the Uniform sample. This trend is borne out in Fig. 4(a) since the pulse durations are around 5.5 ms (Uniform) and 10 ms (Graded). The DIC images in Fig. 4(b) also confirm that the Uniform metastructure exhibits bimodal buckling of the vertical beams, thus resisting

the favorable unimodal buckling trend that the Graded sample reveals in Fig. 4(c), associated with enhanced shock reduction and prolonged pulse duration. The inset in Fig. 4(a) also reveals the enhanced effectiveness of the unimodal collapse to mitigate the impulse. For the Graded metastructure, it is observed that 27% of the impulse is reduced whereas the Uniform sample only reduces 0.6% of the impulse, showing that the lack of unimodal buckling results in mostly conservative transmission of the impulse like a solid.

At more extreme amplitudes of the impact force around 650 N, Fig. 4(d) shows that the transmitted force amplitude through the Graded metastructure is much higher than that for the Uniform sample. Under this condition, the Graded material fully compacts to a solid while the Uniform metastructure remains slightly less than solidified after the unimodal buckling behavior is induced. The significance of these contrasting behaviors is that the compaction in the Graded metastructure permits a nearly conservative transmission of shock over a short duration of time (5 ms) while the Uniform material prolongs the shock transmission (10 ms) via the longer passage through the several buckling events of the vertical beam network. The net impulse passed by the materials is reduced by 7% for the Uniform material while the Graded metastructure entirely conserves the impulse. The DIC results in Fig. 4(e,f) respectively for the Uniform and Graded metastructures show that by 3 ms the Uniform material has not yet transitioned to unimodal buckling whereas the Graded metastructure has exhausted most of the collapse sequence and is nearly solidified. Video 4 contrasts all six impact events captured for the Uniform and Graded metastructures studied here: 3 shock amplitudes per sample. The videos are synchronized with the start of impact to explicitly illuminate the relative rates by which internal dynamics and collapse occur.

Using the high speed video, DIC results, and measurements of transmitted and impact forces, this research discovers that shock mitigation through dissipative metastructures is distinctively defined by mechanisms related to the cross-section design. There is no correlation between the critical forces in the mechanical properties Fig. 1(d) and the capacity of the metastructure to reduce the amplitude or prolong the temporal duration of the transmitted force, Fig. 1(c,f). In fact, these latter dynamic capabilities are found to be governed through the transient nature of collapse stimulated by the metastructure cross-section microstructure design. The uniformity of vertical beam thickness promotes bimodal collapse as a step prior to unimodal collapse, which occurs only for sufficiently great impact force amplitudes. By contrast, the yielding of the Graded metastructure to the unimodal buckling and collapse phenomena is prime to mitigate shock by virtue of the high local shear and y-normal strain in the vertical beams.
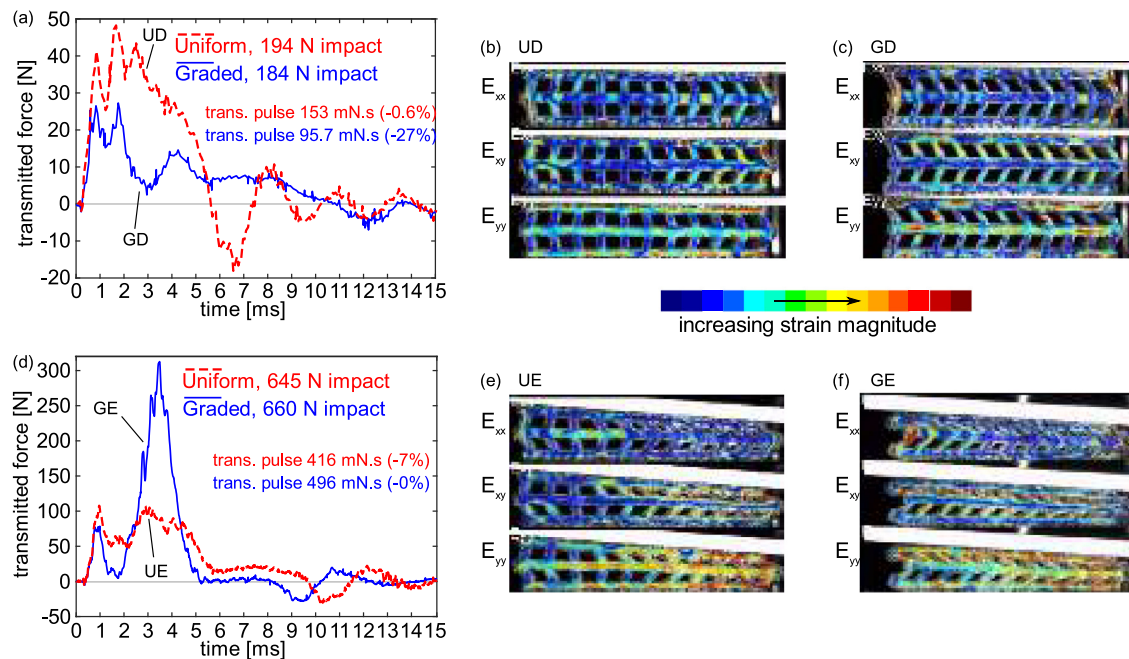
Fig. 4. Low and high amplitude impact force response behaviors for metastructures. (a,d) Transient transmitted force. Inset shows the impulse reduction per sample. DIC results of strain magnitude components for (b,e) Uniform and (c,f) Graded metastructures.

Yet, this mechanism has a limit on the upper amplitude of force for which it may benefit shock reduction. Total compaction or solidification of the metastructure defines the upper limit on the exceptional shock mitigation capacity of the materials, which explains the sudden change of slope in the transmitted force profile for the Graded metastructure around 350 N in Fig. 1(c). These behaviors are reversible and repeatable in this class of thermoset elastomers, although new analyses may be necessary for thermoplastics and other more viscous solids. The overall results of this work suggest that characterizing energy absorption and shock mitigation in viscoelastic metastructures necessitates leveraging principles from dynamic stability of structures [32] rather than solely from structural mechanics [36]. Thus, while innovative material concepts may be created with remarkable mechanical properties suggested for energy absorption, wholly new investigations are required to characterize the suitability of such metastructures to tailor shock.

Declaration of competing interest

The authors declare that they have no known competing financial interests or personal relationships that could have appeared to influence the work reported in this paper.

Acknowledgments

Appendix A. Supplementary data

Supplementary material related to this article can be found online at https://doi.org/10.1016/j.eml.2020.100682.

References

[1] M.R. Haberman, M.D. Guild, Acoustic metamaterials, Phys. Today 69 (2016) 42–48.

[2] M. Thota, S. Li, K.W. Wang, Lattice reconfiguration and phononic band-gap adaptation via origami folding, Phys. Rev. B 95 (2017) 064307.

[3] O.R. Bilal, D. Ballagi, C. Daraio, Architected lattices for simultaneous broadband attenuation of airborne sound and mechanical vibrations in all directions, Phys. Rev. A 10 (2018) 054060.

[4] B.I. Popa, L. Zigoneanu, S.A. Cummer, Experimental acoustic ground cloak in air, Phys. Rev. Lett. 106 (2011) 253901.

[5] A.N. Norris, Acoustic cloaking theory, Proc. R. Soc. Lond. Ser. A Math. Phys. Eng. Sci. 464 (2008) 2411–2434.

[6] T.W. Liu, F. Semperlotti, Tunable acoustic valley-hall edge states in reconfigurable phononic elastic waveguides, Phys. Rev. A 9 (2018) 014001.

[7] J. Paulose, B.G. Chen, V. Vitelli, Topological modes bound to dislocations in mechanical metamaterials, Nat. Phys. 11 (2015) 153–156.

[8] H. Nassar, H. Chen, A.N. Norris, M.R. Haberman, G.L. Huang, Non-reciprocal wave propagation in modulated elastic metamaterials, Proc. R. Soc. Lond. Ser. A Math. Phys. Eng. Sci. 473 (2017) 20170188.

[9] R. Fleury, D. Sounas, M.R. Haberman, A. Alú, Nonreciprocal acoustics, Acoust. Today 11 (2015) 14–21.

[10] Z. Wu, R.L. Harne, K.W. Wang, Exploring a modular adaptive metastructure concept inspired by muscle's cross-bridge, J. Intell. Mater. Syst. Struct. (2015) http://dx.doi.org/10.1177/1045389X15586451.

[11] K.H. Matlack, A. Bauhofer, S. Krödel, A. Palermo, C. Daraio, Composite 3D-printed metastructures for low-frequency and broadband vibration absorption, Proc. Natl. Acad. Sci. 113 (2016) 8386–8390.

[12] V. Neûerka, M. Somr, T. Janda, J. Vorel, M. Doökár, J. Antoö, J. Zeman, J. Novák, A jigsaw puzzle metamaterial concept, Compos. Struct. 202 (2018) 1275–1279.

[13] E. Baravelli, M. Ruzzene, Internally resonating lattices for bandgap generation and low-frequency vibration control, J. Sound Vib. 332 (2013) 6562–6579.

[14] J.D. Hobeck, C.M.V. Laurent, D.J. Inman, 3D printing of metastructures for passive broadband vibration suppression, in: Proceedings of the 20th International Conference on Composite Materials, Copenhagen, Denmark, 2015, pp. 1–9.

[15] P. Vuyk, S. Cui, R.L. Harne, Illuminating origins of impact energy dissipation in mechanical metamaterials, Adv. Energy Mater. 20 (2018) 1700828.

[16] M. Schaeffer, M. Ruzzene, Dynamic reconfiguration of magnto-elastic lattices, C. R. Mec. 343 (2015) 670–679.

[17] S. Shan, S.H. Kang, J.R. Raney, P. Wang, L. Fang, F. Candido, J.A. Lewis, K. Bertoldi, Multistable architected materials for trapping elastic strain energy, Adv. Mater. 27 (2015) 4296–4301.

[18] T. Cohen, S. Givli, Dynamics of a discrete chain of bi-stable elements: a biomimetic shock absorbing mechanism, J. Mech. Phys. Solids 64 (2014) 426–439.

[19] S. Yuan, C.K. Chua, K. Zhou, 3D-printed mechanical metamaterials with high energy absorption, Adv. Mater. Technol. 4 (2019) 1800419.

[20] X. Tan, B. Wang, S. Chen, S. Zhu, Y. Sun, A novel cylindrical negative stiffness structure for shock isolation, Compos. Struct. 214 (2019) 397–405.

[21] R. Lakes, Viscoelastic Materials, Cambridge University Press, Cambridge, 2009.

[22] H. Chen, M.V. Barnhart, Y.Y. Chen, G.L. Huang, Elastic metamaterials for blast wave impact mitigation, in: S. Gopalakrishnan, Y. Rajapakse (Eds.), Blast Mitigation Strategies in Marine Composite and Sandwich Structures, Springer, New York, 2018.

[23] D.M.J. Dykstra, J. Busink, B. Ennis, C. Coulais, Viscoelastic metamaterials. arXiv:1904.11888v1.

[24] C. Yang, M. Boorugu, A. Dopp, J. Ren, R. Martin, D. Han, W. Choi, H. Lee, 4d printing reconfigurable, deployable and mechanically tunable metamaterials, Mater. Horiz. 6 (2019) 1244–1250.

[25] K. Che, C. Yuan, H.J. Qi, J. Meaud, Viscoelastic multistable architected materials with temperature-dependent snapping sequence, Soft Matter 14 (2018) 2492–2499.

[26] N.G. McCrum, C.P. Buckley, C.B. Bucknall, Principles of Polymer Engineering, Oxford University Press, Oxford, 1997.

[27] B. Florijn, C. Coulais, M. van Hecke, Programmable mechanical metamaterials, Phys. Rev. Lett. 113 (2014) 175503.

[28] S. Cui, R.L. Harne, Characterizing the nonlinear response of elastomeric material systems under critical point constraints, Int. J. Solids Struct. 135 (2018) 197–207.

[29] L.E. Kinsler, A.R. Frey, A.B. Coppens, J.V. Sanders, Fundamentals of Acoustics, John Wiley and Sons, New York, 2000.

[30] J. Versace, A review of the severity index, SAE Int. (1971) 710881.

[31] S. Goyal, G.W. Elko, E.K. Buratynski, Role of shock response spectrum in electronic product suspension design, Int. J. Microcircuits Electron. Packag. 23 (2000) 182–190.

[32] G.J. Simitses, Dynamic Stability of Suddenly Loaded Structures, Springer, New York, 1990.

[33] F. Pan, Y. Li, Z. Li, J. Yang, B. Liu, Y. Chen, 3D pixel mechanical metamaterials, Adv. Mater. (2019) 1900548.

[34] H. Yazdani Sarvestani, A.H. Akbarzadeh, A. Mirbolghasemi, K. Hermenean, 3D printed meta-sandwich structures: failure mechanism, energy absorption and multi-hit capability, Mater. Des. 160 (2018) 179–193.

[35] C.R. McInnes, T.J. Waters, Reconfiguring smart structures using phase space connections, Smart Mater. Struct. 17 (2008) 025030.

[36] Z.P. Baûant, L. Cedolin, Stability of Structures: Elastic, Inelastic, Fracture, and Damage Theories, World Scientific Publishing Co., Hackensack, New Jersey, 2010.